Rekha Panchal, Sanjeev Sharma

ANALYTICAL SOLUTION FOR CREEP DEFORMATION OF FUNCTIONALLY GRADED ORTHOTROPIC CYLINDER UNDER MECHANICAL AND CENTRIFUGAL LOADS

ANALITIČKO REŠENJE DEFORMACIJE PUZANJA FUNKCIONALNOG KOMPOZITNOG ORTOTROPNOG CILINDRA POD MEHANIČKIM I CENTRIFUGALNIM OPTEREĆENJEM

Originalni naučni rad / Original scientific paper
UDK /UDC:

Rad primljen / Paper received: 7.08.2020

Adresa autora / Author's address:
Department of Mathematics, Jaypee Institute of Information Technology, Noida, India
email: rekhapanchalmath@gmail.com ; sanjiit12@rediffmail.com

Keywords
- cylinder
- creep
- orthotropic
- pressure
- functionally graded material (FGM)

Abstract

This work intends to introduce an analytical solution for determining steady state creep stresses in thick hollow cylinder under centrifugal and mechanical loads. The solution is based on generalized strain measures. Asymptotic solution is obtained at critical points of the nonlinear differential equation defining deformed state using Seth's transition theory. The advantage of this method is that it overcomes the incompressibility condition in classical theory and also any type of the physical problem can be solved without using creep strain law or jump conditions. The inhomogeneity in the cylinder is assumed to vary radially according to power law. In this problem, the effect of anisotropy, non-homogeneity and rotation on thick hollow cylinder has been investigated for three materials. The results are compared with the previous work and help to attain better agreement between experimental and theoretical results. The main result of this study is that, by applying a suitable angular velocity and non-homogeneity parameter, the distributions of mechanical displacement and mechanical stresses can be controlled.

Ključne reči
- cilindar
- puzanje
- ortotropan
- pritisak
- funkcionalni kompozitni materijal (FGM)

Izvod

U radu je prezentovano analitičko rešenje za određivanje napona stacionarnog puzanja kod debelog šupljeg cilindra, pod dejstvom centrifugalnog i mehaničkog opterećenja. Rešenje se zasniva na generalizovanoj meri deformacija. Asimptotsko rešenje je dobijeno u kritičnim tačkama nelinearne diferencijalne jednačine, kojim se definiše deformisano stanje preko teorije prelaznih napona Seta. Prednost ove metode je što predupređuje uslov nestišljivosti u klasičnoj teoriji i, takođe, bilo koji fizički problem se može rešiti bez primene zakona puzanja ili uslova prekidnog skoka. Pretpostavlja se da nehomogenost u cilindru varira radijalno prema eksponencijalnom zakonu. Kod ovog problema, uticaj anizotropije, nehomogenosti i rotacije na debeli šuplji cilindar su istraženi za tri materijala. Rezultati se upoređeni sa prethodnim radom i doprinose boljem poklapanju teorijskih i eksperimentalnih rezultata. Osnovni rezultat u ovom radu se sastoji u tome da primenom odgovarajuće ugaone brzine i nehomogenog parametra dozvoljava kontrolisanje raspodele mehaničkog pomeranja i napona.

INTRODUCTION

Orthotropic structures are very common in present day engineering. Orthotropic cylinder has gained extensive uses and acceptance and has already earned worldwide popularity in nearly all kinds of applications, housing, marine, highway bridge deck, aerospace and for strengthening of structures. As, we know that large number of real materials often stiffer in one orientation than in other orientations. The area of anisotropic materials is very vast and tough to investigate. Failure of cylinders fabricated of anisotropic material can be fatal to person and surroundings. In this research paper, we study effects of orthotropic materials that differ in stiffness in three orthogonal axes. Therefore, the reliability of the cylinder should be promised. Further, in many of the applications, the material of the cylinders operates at excessive stress and temperature /1/ that cause creep failure. FGMs are basically non-homogeneous composite materials which are extremely heat resistant and with enhanced mechanical properties in engineering fields /2-3/. It is well known that most materials are non-homogeneous due to imperfect manufacturing conditions. Owing to its unique features with applications to many material science and engineering fields, the FGM structure has attracted the interest of researchers and engineers. Bailey creep theory /4/ is proposed for an idealised homogeneous material loaded uniaxially. Betten /5/ mentioned the creep mechanics of cylinders. Bhatnagar et al. /6/ calculated creep stresses and strain rates in homogeneous orthotropic rotating cylinder using Norton's law and concluded that anisotropic material is beneficial for manufacturing purposes because it allows the cylinder to sustain larger forces without a risk of failure under creep. Later on, Zenkour /7/ obtained the analytic solutions for the rotating orthotropic cylinders of variable and uniform thickness and concluded that varying thickness in cylinders shows excellent result. Also, Singh et al. /8/ investigated creep behaviour using Hoffman's yield criterion in an FG thick composite cylinder subjected to internal pressure in the presence of residual stress and concluded that residual stresses have strong influence on creep rates. Also, Manoj et al. /9/ determined solution in closed form for radial and circumferential stresses in FG disk using infinitesimal strain theory. Manoj et al. /10/ obtained analytical solution for two-dimensional FG pressurized cylinder using power series method and analysed numerically. Manoj et al. /11/ analysed the effect of mechanical and thermomechanical stresses on sandwich composition of thick-walled cylinder using finite element analysis. All the above researchers use infinitesimal theory of elasticity. The result obtained using infinitesimal theory is found to be on unsafe side when compared to those obtained using finite strain theory as it neglects the non-linear terms of displacement. Seth's transition theory /12/ act as a benchmark in dealing with the problems of elastic-plastic and creep deformation which has been applied by various researchers, i.e. S.K. Gupta et al. /13/ determined the stresses for orthotropic rotating cylinder. Sharma et al. /14/ investigated the creep stresses in pressurized rotating spherical shell and discusses the impact of inhomogeneity.

However, studies related to creep in pressurized orthotropic thick-walled cylinders fabricated of functionally graded materials are few in number. Thus, a research must be undertaken to study the creep mechanism in an FG orthotropic cylinder under pressure and rotation. In this study, we theoretically analyse the impact of inhomogeneity in the evaluation of creep deformation.

OBJECTIVE OF THE STUDY

The aim is to study the behaviour of rotating thick-walled orthotropic cylinder with varying material properties subjected to pressure. Analysis of yield stress informs the designers a bit more about the safety of the cylinder at the acting pressure. Therefore, our main objective is to analyse allowable elastic-creep stresses in an open-ended FG rotating orthotropic thick hollow cylinder under pressure, to incorporate a 'safety factor' that prevents the pressurized cylinder from bursting and helpful in practical design of orthotropic cylinder.

BASIC FORMULATION OF THE PROBLEM

We now study an open ended axisymmetric thick-walled orthotropic cylinder fabricated of FGM with inside and outside radii a_i and b_0 respectively, under pressure p_{a_i} and p_{b_0}, respectively. Axisymmetric deformations are considered so that u is the only displacement component. The z-axis is considered as axis of rotation. Displacement components in the cylindrical coordinate system are:

$$u_r = r(1-\kappa)\,, \quad u_\theta = 0\,, \quad \text{and} \quad u_z = cz\,, \tag{1}$$

where: κ is defined as a function of r only; and c is defined as a constant.

Generalized strain measure ε_{jj} is defined by Seth as integral of the weighted function

$$\varepsilon_{jj} = \int_0^{\varepsilon_{jj}^A}\left[1-2\varepsilon_{jj}^A\right]^{\frac{n}{2}-1} d\varepsilon_{jj}^A = \frac{1}{n}\left[1-\left(1-2\varepsilon_{jj}^A\right)^{\frac{n}{2}}\right] \quad (j=1,2,3)\,, \tag{2}$$

where: n denotes the measure; and ε_{jj}^A are the Almansi principal components of strain.

Using Eq.(2), the generalized components of strain are

$$\varepsilon_{rr} = \frac{1}{n}\left[1-(r\kappa'+\kappa)^n\right], \quad \varepsilon_{\theta\theta} = \frac{1}{n}[1-\kappa^n]\,,$$
$$\varepsilon_{zz} = \frac{1}{n}[1-(1-d)^n]\,, \quad \varepsilon_{r\theta} = \varepsilon_{\theta z} = \varepsilon_{zr} = 0\,, \tag{3}$$

where: n is nonlinear measure; and $\kappa' = d\kappa/dr$.

Component of stress for orthotropic material is given as

$$\tau_{rr} = C_{11}(n)^{-1}[1-(r\kappa'+\kappa)^n] + C_{12}(n)^{-1}[1-\kappa^n] + C_{13}(n)^{-1}[1-(1-c)^n]$$
$$\tau_{\theta\theta} = C_{21}(n)^{-1}[1-(r\kappa'+\kappa)^n] + C_{22}(n)^{-1}[1-\kappa^n] + C_{23}(n)^{-1}[1-(1-c)^n]$$
$$\tau_{zz} = C_{31}(n)^{-1}[1-(r\kappa'+\kappa)^n] + C_{32}(n)^{-1}[1-\kappa^n] + C_{33}(n)^{-1}[1-(1-c)^n]$$
$$\tau_{r\theta} = \tau_{\theta z} = \tau_{zr} = 0\,, \tag{4}$$

where: τ_{rr}, $\tau_{\theta\theta}$ and τ_{zz} denotes stresses in radial, tangential and axial direction.

FUNCTIONALLY GRADED MATERIAL FORMULATION

Here we take into consideration functionally graded orthotropic material in which material properties vary radially as:

$$C_{ij} = C_{0ij}\left(\frac{r}{b_o}\right)^{-k}, \quad (i, j = 1,2,3) \tag{5}$$

where: $a_i \le r \le b_0$ ($k \le 0$), the subscript $0i,j$ represents corresponding value on the external surface of the functionally graded thick hollow cylinder, and k is power-law index of material non-homogeneity; C_{0ij} is the material property, such as elastic coefficient.

Using Eq.(5) in Eq.(4), we get

$$\tau_{rr} = (n)^{-1}C_{011}\left(\frac{r}{b_0}\right)^{-k}[1-(r\kappa'+\kappa)^n] + (n)^{-1}C_{012}\left(\frac{r}{b_0}\right)^{-k}[1-\kappa^n] +$$
$$+(n)^{-1}C_{013}\left(\frac{r}{b_0}\right)^{-k}[1-(1-c)^n],$$
$$\tau_{\theta\theta} = (n)^{-1}C_{021}\left(\frac{r}{b_0}\right)^{-k}[1-(r\kappa'+\kappa)^n] + (n)^{-1}C_{022}\left(\frac{r}{b_0}\right)^{-k}[1-\kappa^n] +$$
$$+(n)^{-1}C_{023}\left(\frac{r}{b_0}\right)^{-k}[1-(1-c)^n],$$
$$\tau_{zz} = (n)^{-1}C_{031}\left(\frac{r}{b_0}\right)^{-k}[1-(r\kappa'+\kappa)^n] + (n)^{-1}C_{032}\left(\frac{r}{b_0}\right)^{-k}[1-\kappa^n] +$$
$$+(n)^{-1}C_{033}\left(\frac{r}{b_0}\right)^{-k}[1-(1-c)^n],$$
$$\tau_{r\theta} = \tau_{\theta z} = \tau_{zr} = 0\,, \tag{6}$$

where: τ_{ij}, e_{ij} are stress and strain tensors, respectively.

Equation of equilibrium /12/ is given as,

$$\frac{d}{dr}(hr\tau_{rr}) - h\tau_{\theta\theta} + h\rho\omega^2 r^2 = 0\,, \tag{7}$$

where: radial coordinate is denoted by r; radial and tangential or hoop stresses are denoted by τ_{rr} and $\tau_{\theta\theta}$, respectively; wall thickness is denoted by h, the density of the material is denoted by ρ; and angular speed of rotating non-homogeneous cylinder is denoted by ω.

IDENTIFICATION OF TRANSITION POINT

In response to applied loading to a deformable solid, we noticed that the solid body first undergoes elastic deformation. If the loading is further sustained, plastic flow might set in and lead to creep. So, there always exists a transitional state in between elastic and creep state that is identified as transition state, /15/. To clarify the transition from elastic to creep state, firstly, we require to identify transition state as an asymptotic one. Therefore, the differential system describing the elastic state should reach a critical value in the transition state. The nonlinear differential equation for transition state is obtained by substituting Eq.(6) in Eq.(7), as

$$\frac{d\kappa}{d\eta}\left[h\eta(\eta+1)^n+\frac{C_{012}\left(\frac{r}{b_0}\right)^{-k}}{C_{011}\left(\frac{r}{b_0}\right)^{-k}}h\eta-\frac{\rho\omega^2 r^2 h}{nC_{011}\left(\frac{r}{b_0}\right)^{-k}\kappa^n}+\frac{h}{nC_{011}\left(\frac{r}{b_0}\right)^{-k}\kappa^n}\right]\left[\left\{(k-1)C_{011}\left(\frac{r}{b_0}\right)^{-k}+C_{021}\left(\frac{r}{b_0}\right)^{-k}\right\}\left\{1-\kappa^n(\eta+1)^n\right\}+\right.$$

$$\left.+\left\{(k-1)C_{012}\left(\frac{r}{b_0}\right)^{-k}+C_{022}\left(\frac{r}{b_0}\right)^{-k}\right\}\{1-\kappa^n\}+\left\{(k+t-1)C_{013}\left(\frac{r}{b_0}\right)^{-k}+C_{023}\left(\frac{r}{b_0}\right)^{-k}\right\}\left\{1-(1-c)^n\right\}\right]+h\kappa\eta(\eta+1)^{n-1}=0 \qquad (8)$$

where: $r\kappa' = \eta\kappa$.

Transition points /16/ of κ in Eq.(5) are $\eta \to 0$, $\eta \to -1$, and $\eta \to \pm\infty$.

Transition points are basically the critical points of the equation whenever the equation is asymptotically stable and derivates are not differentiable. At this physical point, distinction between elastic and creep state disappears.

Boundary conditions considered are

$$\tau_{rr}=-p_{a_i} \text{ at } r=a_i \text{ and } \tau_{rr}=-p_{b_0} \text{ at } r=b_0. \qquad (9)$$

Resultant of force normal to the plane z = const. must vanish, i.e.

$$\int_{a_i}^{b_0} r\tau_{zz}\,dr=0. \qquad (10)$$

CREEP STRESSES

It has been found /12-15/ that transition function given by principal stress-difference at the transition point $\eta \to -1$ evaluate creep stresses. The transition function TR is defined

$$TR=\tau_{rr}-\tau_{\theta\theta}=(n)^{-1}\Big[(C_{11}-C_{21})\{1-\kappa^n(\eta+1)^n\}+$$

$$+(C_{12}-C_{22})\{1-\kappa^n\}+(C_{13}-C_{23})\{1-(1-c)^n\}\Big]. \qquad (11)$$

We take logarithmic differentiation of Eq.(11) with respect to 'r', and take the asymptotic value as $\eta \to -1$, and integrate, we get

$$TR=AF_1, \qquad (12)$$

where integration of the constant is represented by A and $F_1 = e^{\int X dr}$ and

$$X=\frac{\left(\frac{C_{11}-C_{21}}{C_{11}}\right)\Big[-kC_{11}r^n-nD^nC_{12}-n\rho\omega^2r^{n+2}+r^n\{(k-1)C_{11}+C_{21}\}+\{(k-1)C_{12}+C_{22}\}\{r^n-D^n\}+r^n\{(k-1)C_{13}+C_{23}\}\{1-(1-c)^n\}\Big]+(C_{12}-C_{22})\{nD^n-kr^n+kD^n\}+(C_{13}-C_{23})\{-kr^n+kr^n(1-c)^n\}}{r\Big[(C_{11}-C_{21})r^n+(C_{12}-C_{22})\{r^n-D^n\}+r^n(C_{13}-C_{23})\{1-(1-c)^n\}\Big]}.$$

Using Eq.(12) in Eq.(11), we get

$$\tau_{rr}-\tau_{\theta\theta}=AF_1. \qquad (13)$$

Substituting this in equilibrium Eq.(7), we obtain

$$\tau_{rr}=AF(r)-\frac{\rho\omega^2r^2}{2}+B, \qquad (14)$$

$$\tau_{\theta\theta}=\tau_{rr}-AF_1, \qquad (15)$$

where: $F(r)=\int\frac{F_1}{r}dr$,

$$\tau_{zz}=\frac{C_{32}(\tau_{rr}+\tau_{\theta\theta})}{C_{12}+C_{22}}+A_1, \qquad (16)$$

where:

$$A_1=\left\{C_{31}-\frac{C_{32}(C_{11}+C_{21})}{C_{12}+C_{22}}\right\}+\left\{C_{33}-\frac{C_{32}(C_{13}+C_{23})}{C_{12}+C_{22}}\right\}\varepsilon_{zz}.$$

Using boundary condition Eq.(9) in Eq.(14), we get

$$A=\frac{p_{b_0}-p_{a_i}-\frac{\rho\omega^2(b_0{}^2-a_i{}^2)}{2}}{\int_{a_i}^{b_0}F\,dr},$$

$$B=-p_{b_0}+\left(\frac{p_{b_0}-p_{a_i}-\frac{\rho\omega^2(b_0{}^2-a_i{}^2)}{2}}{\int_{a_i}^{b_0}F\,dr}\right)F(b_0)+\frac{\rho\omega^2b_0{}^2}{2}.$$

Substituting the values obtained above of A and B in Eqs.(14) and Eqs.(15), creep stresses for steady state orthotropic cylinder are given by:

$$\tau_{rr}=-p_{b_0}+\frac{\left\{(p_{a_i}-p_{b_0})+\frac{\rho\omega^2(b_0^2-a_i^2)}{2}\right\}\int_r^{b_0}Fdr}{\int_{a_i}^{b_0}Fdr}+\frac{\rho\omega^2 b_0^2}{2} \quad (17)$$

$$\tau_{\theta\theta}=-p_{b_0}+\frac{\left\{(p_{a_i}-p_{b_0})+\frac{\rho\omega^2(b_0^2-a_i^2)}{2}\right\}\left[\int_r^{b_0}Fdr+e^{\int Xdr}\right]}{\int_{a_i}^{b_0}Fdr}+\frac{\rho\omega^2(b_0^2-r^2)}{2}. \quad (18)$$

Taking into account the following dimensionless quantities as: $R = r/b_0$, $R_0 = a_i/b_0$, $\sigma_{rr} = \tau_{rr}/C_{011}$, $\sigma_{\theta\theta} = \tau_{\theta\theta}/C_{011}$, $\sigma_{zz} = \tau_{zz}/C_{011}$, $\Omega^2 = \rho\omega^2 b_0^2/C_{011}$.

Inserting the above dimensionless form of radial, hoop, or circumferential and axial creep stresses for FG orthotropic cylinder given by Eq.(17), Eq.(18) can be rewritten as

$$\sigma_{rr}=-P_{b_0}+\left\{P_{a_i}-P_{b_0}+\frac{\Omega^2(1-R_0^2)}{2}\right\}\frac{\int_R^1 F_2dR}{\int_{R_0}^1 F_2dR}+\frac{\Omega^2(1-R^2)}{2}, \quad (19)$$

where: $F_2(r)=\int\frac{F_1}{b_0R}e^{b_0\int X_1dR}dR$,

$$X_1=\frac{\left(\frac{C_{11}-C_{21}}{C_{11}}\right)\left(-kC_{11}-\frac{nD^n}{b_0^nR^n}C_{12}-n\rho\omega^2b_0^2R^2+\{(k-1)C_{11}+C_{21}\}+\{(k-1)C_{12}+C_{22}\}\left\{1-\frac{D^n}{b_0^nR^n}\right\}+\{(k-1)C_{13}+C_{23}\}\{1-(1-c)^n\}+\right.}{b_oR\left[(C_{11}-C_{21})+(C_{12}-C_{22})\left\{1-\frac{D^n}{b_0^nR^n}\right\}+r^n(C_{13}-C_{23})\{1-(1-d)^n\}\right]}$$

$$\frac{\left.+(C_{12}-C_{22})\left(\frac{nD^n}{b_0^nR^n}-k\left\{1-\frac{D^n}{b_0^nR^n}\right\}\right)-k(C_{13}-C_{23})\{1-(1-c)^n\}\right)}{},$$

$$\sigma_{\theta\theta}=-P_{b_0}+\left\{P_{a_i}-P_{b_0}+\frac{\Omega^2(1-R_0^2)}{2}\right\}\frac{\int_R^1 F_2dR}{\int_{R_0}^1 F_2dR}\left[\int_R^1 b_0F_2dR+e^{b_0\int X_2dR}\right]+\frac{\Omega^2(1-R^2)}{2}, \quad (20)$$

$$\sigma_{zz}=\frac{C_{32}(\sigma_{rr}+\sigma_{\theta\theta})}{C_{12}+C_{22}}+\left\{C_{31}-\frac{C_{32}(C_{11}+C_{21})}{C_{12}+C_{22}}\right\}+\left\{C_{33}-\frac{C_{32}(C_{13}+C_{23})}{C_{12}+C_{22}}\right\}\varepsilon_{zz}^*. \quad (21)$$

RESULTS AND DISCUSSION

In order to compute the numerical results, an orthotropic and isotropic cylinder fabricated of FGM is considered with plain strain assumption. The inside and outside radius of the cylinder are considered as $a_i = 1$ and $b_0 = 2$, respectively. Compressibility which is one of the mechanical properties of the cylinder is presumed to be changing through the radius. Material property of the cylinder fabricated of FG orthotropic material (barite and uranium (alpha)) and isotropic material (steel) are shown in Table 1.

Table 1. Elastic constants C_{ij} used (in units of 10^{11} N/m^2).

Materials	C_{11}	C_{12}	C_{13}	C_{21}	C_{22}	C_{23}	ρ
steel (isotropic)	5.326	3.688	3.688	3.688	5.326	3.688	7.8
barite (orthotropic)	0.8941	0.4614	0.2691	0.4614	0.7842	0.2676	4.4
uranium (alpha) (orthotropic)	2.1486	0.4622	0.2176	0.4622	1.9983	1.0764	19.0

Table 2.1. Creep stresses for FGM cylinder fabricated of barite material with $P_{a_i} = 3$, $P_{b0} = 1$ and $P_{a_i} = 1$, $P_{b0} = 3$.

$\sigma_{\theta\theta}$			$N = 3$			$N = 5$		
pressure	angular velocity	k/R	0.5	0.7	0.9	0.5	0.7	0.9
$P_{a_i} > P_{b0}$	0.7	-2	10.12	5.32	1.24	6.81	2.83	0.21
		-3	23.23	15.52	5.77	6.80	2.80	0.23
	1	-2	18.91	10.47	3.09	13.38	6.3	1.37
		-3	40.81	27.51	10.65	13.37	6.26	1.4
	1.3	-2	30.79	17.44	5.59	22.28	11.01	2.93
		-3	193.05	131.39	53.74	22.20	10.93	2.98
$P_{b0} > P_{a_i}$	0.7	-2	2.78	0.57	-1.7	1.82	-0.14	-1.99
		-3	6.55	3.5	-0.39	8.39	-0.15	-1.99
	1	-2	11.57	5.72	0.14	8.39	3.33	-0.84
		-3	24.13	15.49	4.47	17.24	3.311	-0.82
	1.3	-2	23.46	12.68	2.64	17.29	8.04	8.049
		-3	140.88	95.15	37.48	1.82	7.99	0.75

Table 2.2. Creep stresses for FGM cylinder fabricated of uranium (alpha) material with P_{ai} = 3, P_{b0} = 1 and P_{ai} = 1, P_{b0} = 3.

$\sigma_{\theta\theta}$			N = 3			N = 5		
pressure	angular velocity	k/R	0.5	0.7	0.9	0.5	0.7	0.9
$P_{ai} > P_{b0}$	0.7	-2	18.11	10.26	3.1	12.062	5.53	1.09
		-3	59.3	41.99	17.02	12.88	5.58	1.07
	1	-2	34.93	20.32	6.77	24.06	11.81	3.17
		-3	108.91	77.31	31.78	25.53	11.9	3.12
	1.3	-2	57.38	33.92	11.73	40.28	20.32	5.97
		-3	841.12	601.86	254.23	43.94	20.83	5.98
$P_{b0} > P_{ai}$	0.7	-2	10.19	5.05	-0.05	6.98	2.54	-1.11
		-3	32.03	21.87	7.33	7.42	2.57	-1.13
	1	-2	27.01	15.1	3.61	18.98	8.82	0.96
		-3	81.64	57.19	22.09	20.07	8.89	0.92
	1.3	-2	49.76	28.7	8.58	35.2	17.33	3.76
		-3	705.1	503.78	211.43	38.27	17.76	3.76

Table 2.3. Creep stresses for FGM cylinder fabricated of steel material with P_{ai} = 3, P_{b0} = 1 and P_{ai} = 1, P_{b0} = 3.

$\sigma_{\theta\theta}$			N = 3			N = 5		
pressure	angular velocity	k/R	0.5	0.7	0.9	0.5	0.7	0.9
$P_{ai} > P_{b0}$	0.7	-2	3.82	1.55	-0.13	2.39	0.49	-0.56
		-3	8.6	5.37	1.59	2.24	0.47	-0.52
	1	-2	6.32	2.99	0.36	4.36	1.53	-0.21
		-3	12.85	8.19	2.72	4.15	1.52	-0.17
	1.3	-2	9.7	4.92	1.04	7.03	2.94	0.25
		-3	48.59	31.84	12.43	6.64	2.88	0.3
$P_{b0} > P_{ai}$	0.7	-2	-3.03	-2.8	-2.9	-2.6	-2.48	-2.77
		-3	-4.45	-3.93	-3.41	-2.55	-2.48	-2.78
	1	-2	-0.53	-1.37	-2.39	-0.63	-1.44	-2.43
		-3	-0.21	-1.11	-2.28	-0.64	-1.45	-2.42
	1.3	-2	2.84	0.56	-1.72	2.04	-0.03	-1.96
		-3	14.61	8.71	1.72	1.92	-0.05	-1.94

To see the effect of many parameters i.e. finite strain measure $N = (n)^{-1}$, inside pressure P_{ai} and outside pressure P_{b0} on thick-walled rotating cylinder fabricated of FGM (barite, uranium (alpha), and steel), Table 1, Table 2, and the graphs have been plotted among radii ratio and creep stresses for different pressure under centrifugal force. The angular velocity with which cylinder rotates is 0.5, 1.

The results are presented in a non-dimensional form. The distribution of creep stresses at different angular velocity for different materials with linear strain measure are drawn in Fig. 1. It seems from Fig. 1 that for linear measure, the creep stresses in the cylinder fabricated of homogeneous material increases as compared to the cylinder composed of non-homogeneous material. Moreover, circumferential stresses are maximum at inner surface, and tensile. It can be seen that the circumferential creep stress decreases with decrease in angular velocity. However, for high FG cylinder, these creep stresses are less as compared to the less FG cylinder. Creep stresses for isotropic material steel are less as compared to orthotropic material barite and uranium (alpha). The results for the creep stresses of circular cylinder with linear strain measure are compared with those of nonlinear strain measure in Figs. 1-4. According to results plotted in Fig. 2, circumferential creep stresses are maximum for less FG orthotropic material as compared to the homogeneous orthotropic cylinder with nonlinear strain measure. Also, it has been noticed that circumferential creep stresses are maximum for cylinder fabricated of isotropic FGM as compared to orthotropic FGM or homogeneous material. It is noticed that with the consideration of nonlinearity, the outcomes are better, because in case of classical theory, this nonlinear transition region through which in actual yield occur is neglected and creep strains are never linear. In the transition state, entire material is participating, not merely a particular region or line, as is presumed by classical theories. A recent numerical investigation /16/ on the flow and deformation theories, additionally shows that a continuous approximation through a transition region ends up satisfactory as well as a convergent solution.

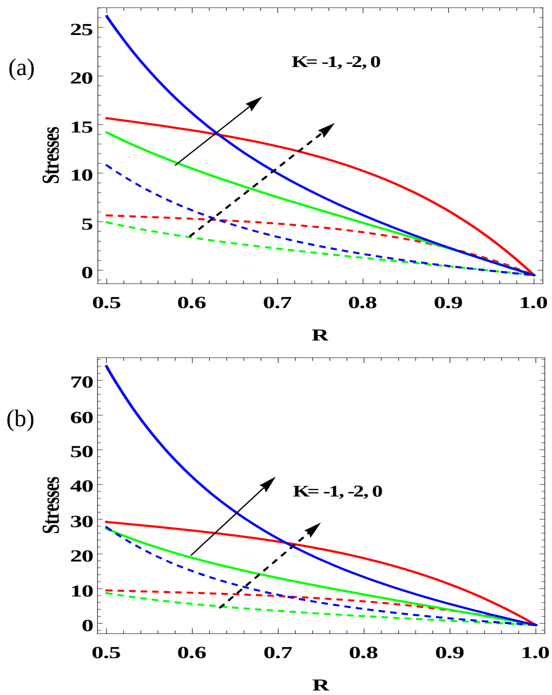

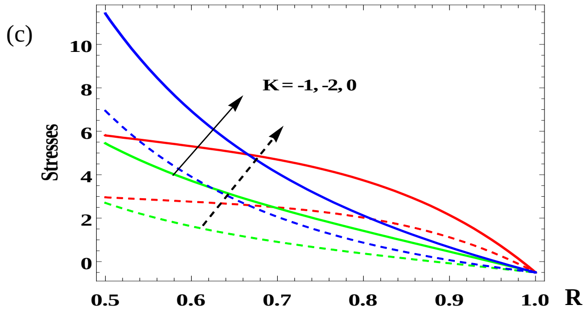

Figure 1. Creep stress of dissimilar materials: a) barite; b) uranium (alpha); c) steel; for non-homogeneity parameter K with $P_{a_i} = 4$, $P_{b_0} = 0.5$, $N = 1$, where solid and dashed lines respectively represent angular velocity $\Omega^2 = 1$ and 0.5.

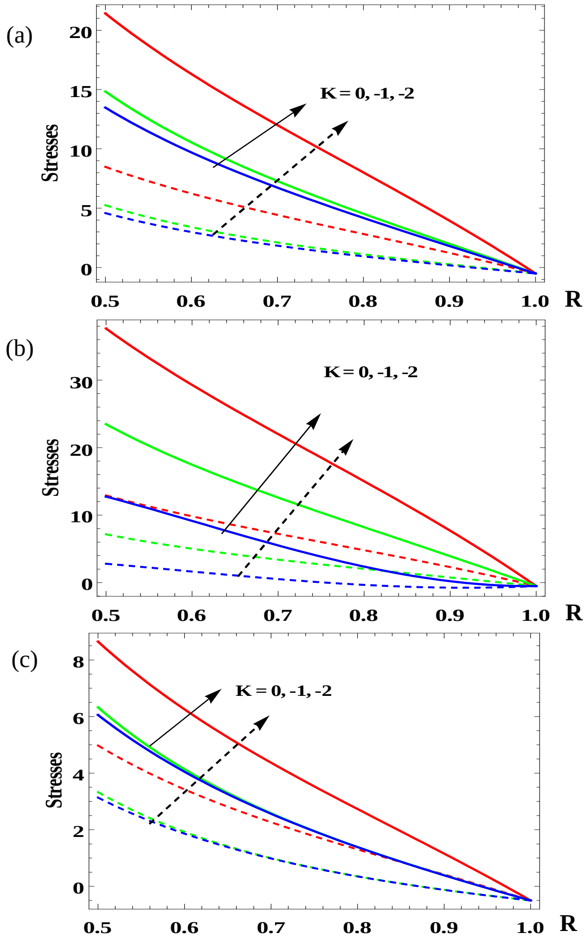

Figure 2. Creep stress of dissimilar materials: a) barite; b) uranium (alpha); c) steel; for non-homogeneity parameters K with $P_{a_i} = 4$, $P_{b_0} = 0.5$, $N = 3$, where solid and dashed lines respectively represent angular velocity $\Omega^2 = 1$ and 0.5.

In a like manner, the distribution of the creep stress in the cylinder is shown in Fig. 3. For nonlinear measure, the homogeneous orthotropic cylinder has less circumferential creep stresses as compared to high or less FG cylinder, as illustrated in Fig. 4. We see creep stresses increase at inner surface, while they decrease at outer surface. To clarify the effect of pressure, Figs. 3 and 4 are presented.

The results of Figs. 1 to 4 can be summarized as follows:

– Creep stresses of the cylinder under pressure are tensile in nature.
– Cylinder subjected to pressure and centrifugal loading shows different behaviour as we consider linear and non-linear strain measure.
– Angular velocity has considerable effect on the displacements and creep stresses in the cylinder.
– In the cylinder, the creep stress rises with increase in the value of inside pressure.
– The non-homogeneity parameter is highly effective under the inside and outside pressures to tailor the mechanical properties of the material.

Influence of measure and non-homogeneity on the creep stresses is shown in Tables 2.1, 2.2 and 2.3. It is noticed that creep stresses are tensile and are maximal at inner surface with nonlinear measure, as can be noticed from the Tables 2.1, 2.2 and 2.3. It is also observed that with the decrease in nonlinearity, the creep stress increases. It is observed from Table 2.1 that creep stresses are maximum for the cylinder fabricated of less non-homogenous material and are high for the cylinder fabricated of highly non-homogeneous material. Also, with the increase of angular velocity, the creep stress increases. When the inside pressure is more than the outside pressure, the stresses are tensile but when the inside pressure is less than outside pressure, these stresses become compressive from tensile, as illustrated in Tables 2.1, 2.2 and 2.3.

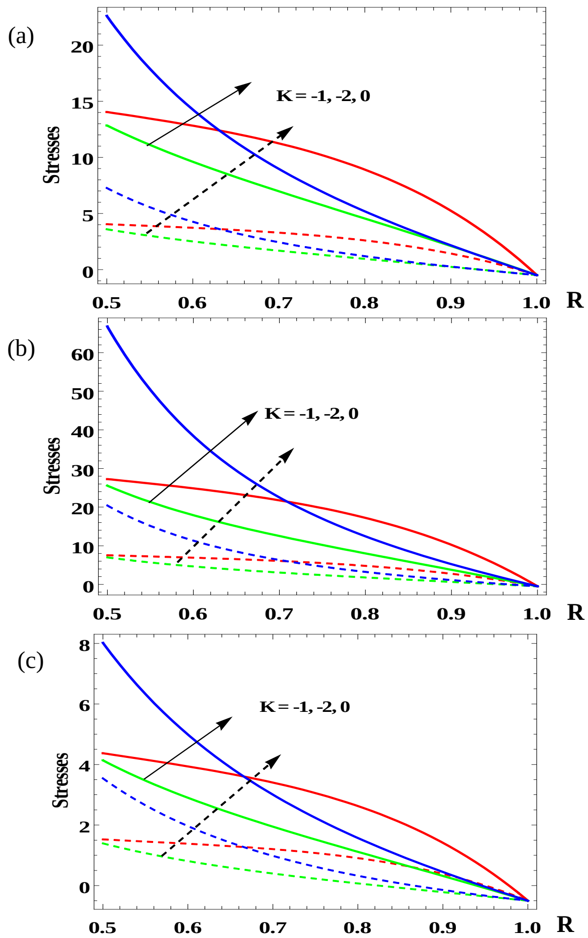

Figure 3. Creep stress of dissimilar materials: a) barite; b) uranium (alpha); c) steel; for non-homogeneity parameter K with $P_{a_i} = 2$, $P_{b_0} = 0.5$, $N = 1$, where solid and dashed lines respectively represent angular velocity $\Omega^2 = 1$ and 0.5.

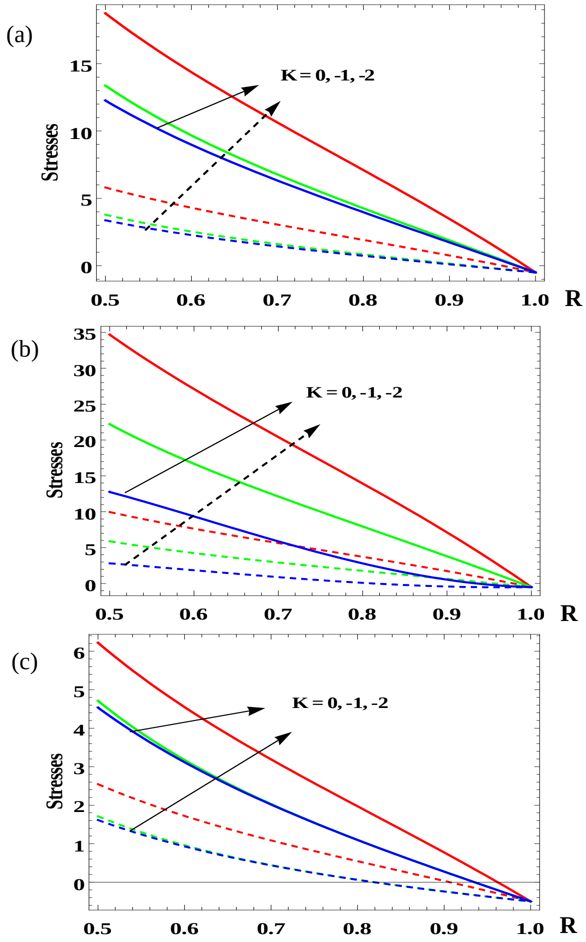

Figure 4. Creep stress of dissimilar materials: a) barite; b) uranium (alpha); c) steel; for variable non-homogeneity parameter K with $P_{a_i} = 2$, $P_{b0} = 0.5$, $N = 3$, where solid and dashed lines respectively represent angular velocity $\Omega^2 = 1$ and 0.5.

It has been noticed from Table 2.2 that circumferential creep stresses are maximum at the inner surface of rotating cylinder when inside pressure is more than outside pressure, for angular speed 1.3. With increase in non-homogeneity, these creep stresses further decrease. It can be observed that at outside surface these stresses become compressive from tensile. Also, when the inside pressure is less than outside pressure, the creep stress become compressive. From Tables 2.2 and 2.3 it is also noticed that circumferential or tangential creep stresses are less for highly non-homogeneous rotating cylinder, and these creep stresses increase with the decrease in non-homogeneity. Also, circumferential creep stresses are high for orthotropic material, i.e. uranium (alpha) as compared to orthotropic material, i.e. barite and isotropic material, i.e. steel. From Tables 2.1, 2.2 and 2.3, it can be observed that with the increase in measure, circumferential creep stresses decrease significantly.

CONCLUSIONS

On the basis of above discussion, conclusion revealed that circular cylinder fabricated of homogeneous isotropic material (steel) under pressure with nonlinear measure is a better choice for designing, as compared to cylinder fabricated of FG orthotropic material (barite) and orthotropic material (uranium). It is due to the reason that circumferential or hoop stresses are less for steel as compared to barite and uranium. Cylinder with less angular velocity is safer for design. This helps in stress savings, thus minimizes the chances of fracture of cylinder, due to inside and outside pressure.

REFERENCES

1. Erdogan, F. (1995), *Fracture mechanics of functionally graded materials*, Comp. Eng. 5(7): 753-770. doi: 10.1016/0961-9526(95)00029-M
2. Suresh, S., Mortensen, A., Fundamentals of Functionally Graded Materials: Processing and Thermomechanical Behavior of Graded Metals and Metal-Ceramic Composites, IOM Comm. Ltd., London, UK, 1998.
3. Reddy, J.N. (2000), *Analysis of functionally graded plates*, Int. J Num. Methods Eng. 47(1-3): 663-684. doi: 10.1002/(SICI)1097-0207(20000110/30)47:1/3<663::AID-NME787>3.0.CO;2-8
4. Bailey, R.W. (1935), *Utilization of creep test data in engineering design*, Proc. Inst. Mech. Engrs. 131(1): 131-349. doi: 10.1243/PIME_PROC_1935_131_012_02
5. Betten, J., Creep Mechanics, 3rd Ed., Springer-Verlag Berlin Heidelberg, 2008. doi: 10.1007/978-3-540-85051-9
6. Bhatnagar, N.S., Arya, V.K., Debnath, K.K. (1980), *Creep analysis of orthotropic rotating cylinder*, J Pres. Ves. Tech. 102(4): 371-377. doi: 10.1115/1.3263347
7. Zenkour, A.M. (2006), *Rotating variable-thickness orthotropic cylinder containing a solid core of uniform-thickness*, Arch. Appl. Mech. 76: 89-102. doi: 10.1007/s00419-006-0007-y
8. Singh, T., Gupta, V.K. (2013), *Modeling steady state creep behavior of functionally graded thick cylinder in the presence of residual stress*, Procedia Eng. 55: 760-767. doi: 10.1016/j.proeng.2013.03.328
9. Sahni, M., Sahni, R. (2015), *Rotating functionally graded disc with variable thickness profile and external pressure*, Procedia Comp. Sci. 57: 1249-1254. doi: 10.1016/j.procs.2015.07.426
10. Kumar, S., Sahni, M. (2019), *Two-dimensional mechanical stresses for a pressurized cylinder made of functionally graded material*, Struct. Integ. and Life, 19(2): 79-85.
11. Mehta, P.D., Mishra, L., Sahni, M. (2019), *Thermomechanical stress analysis of thick-walled cylinder with inner FGM layer*, Struct. Integ. and Life, 19(3): 211-223.
12. Seth, B.R. (1970), *Transition conditions: The yield conditions*, Int. J Non-Linear Mech. 5(2): 279-285. doi.org/10.1016/0020-7462(70)90025-9
13. Gupta, S.K., Bhardwaj, P.C. (1986), *Elastic plastic and creep transition in orthotropic rotating cylinder*, Proc. Ind. Nat. Sci. Acad. 52(6A): 1357-1369.
14. Sharma, S., Panchal, R. (2017), *Thermal creep deformation in pressurized thick-walled functionally graded rotating spherical shell*, Int. J Pure Appl. Math. 114(3): 435-444. doi: 10.12732/ijpam.v114i3.2
15. Borah, B.N. (2005), *Thermo-elastic-plastic transition*, Mathematical studies in nonlinear wave propagation, Contemp. Math. 379: 93-111. doi: 10.1090/conm/379
16. Bragg, L. (1942), *A theory of the strength of metals*, Nature, 149: 511-513. doi: 10.1038/149511a0